

PAPER • OPEN ACCESS

## Evaluation of progressive damage of discontinuity asperities due to shearing by means photogrammetric survey

To cite this article: M T Carriero *et al* 2023 *IOP Conf. Ser.: Earth Environ. Sci.* **1124** 012053

View the [article online](#) for updates and enhancements.

You may also like

- [Challenging multi-sensor data models and use of 360 images. The Twelve Months Fountain of Valentino park in Turin.](#)  
L Teppati Losè, G Sammartano, F Chiabrando et al.
- [Novel system for the automatization of photogrammetric data capture for metrological tasks: application to study of gears](#)  
M Rodríguez and P Rodríguez
- [A generic approach for photogrammetric survey using a six-rotor unmanned aerial vehicle](#)  
K N Tahar, A Ahmad, W A A W M Akib et al.

### ECS Toyota Young Investigator Fellowship



For young professionals and scholars pursuing research in batteries, fuel cells and hydrogen, and future sustainable technologies.

At least one \$50,000 fellowship is available annually.  
More than \$1.4 million awarded since 2015!



Application deadline: January 31, 2023

**Learn more. Apply today!**

# Evaluation of progressive damage of discontinuity asperities due to shearing by means photogrammetric survey

M T Carriero<sup>1</sup>, A M Ferrero<sup>2</sup>, M R Migliazza<sup>1</sup>, G Umili<sup>2</sup>

<sup>1</sup>Department of Structural, Geotechnical and Building Engineering, Polytechnic of Turin, Corso Duca degli Abruzzi 24, 10129 Turin, Italy

<sup>2</sup>Department of Earth Sciences, University of Turin, via Valperga Caluso 35, 10125 Turin, Italy

mtcarriero@hotmail.it

**Abstract.** It is well known that the mechanical behaviour of rock discontinuities strongly influences the stability of slopes and fractured rock walls. With this end, particular attention must be paid to the analysis of the roughness of natural discontinuities, which represents a peculiar geometric feature strongly influencing their shear strength. The paper describes an experimental procedure carried out at laboratory scale on natural rock discontinuities to measure the shear strength and the roughness of their surfaces to analyse the progressive damage of the asperities during shearing process. The direct shear tests along discontinuities were coupled to photogrammetric surveys of the surfaces carried out before the tests (natural surfaces), after the first cycle and at the end of the last cycle. This allowed the reconstruction of the digital surface models of the intact and degraded surfaces. Through analytical procedures, the data obtained were processed to obtain geometric descriptors and adequately estimate the Joint Roughness Coefficient (JRC), analysing several profiles extracted along the direction in which the mechanical tests were conducted. The comparison between the experimental results and the roughness surface direct measure showed that discontinuities, even at the small scale, have an inhomogeneous roughness and that discontinuity degree of damage is a progressive process influenced by the state of confinement applied during the tests.

## 1. Introduction

The mechanical and deformation behaviour of a rock mass is directly governed by its degree of fracture, and it is characterized not only by the intact rock characteristics but also by the orientation, geometry and roughness of the rock joints. Understanding the jointed rock mass behaviour is a key element in many engineering applications regarding both rock mass slope stability problems and underground excavations. In the literature, many constitutive models [1,2] have been proposed to understand the shear joint behaviour which depends on different parameters, including normal stress [3], size and scale of the joint [4], surface roughness [1,2], mineral composition [5], surface conditions [6] and mechanical properties [2]. The surface damage can influence the mechanical and hydraulic properties of fractures so joint surface roughness has essential implications for joint shear behaviour evaluation [7]. To quantify the joint surface roughness, many authors have proposed different methods, such as statistical [8,9], fractal [9,10] and directional methods. The Joint Roughness Coefficient (JRC) [2] is probably the most



common parameter used in the engineering practice for assessing the contribution of joint roughness to the discontinuity shear strength. For this reason, several methods have been proposed to correlate other geometrical roughness parameters to JRC [8,9]. Although there are many techniques to analyse discontinuity surfaces, in this work we focus on the remote 3D characterization techniques and to digital photogrammetry [11].

The paper describes an experimental procedure carried out at laboratory scale on natural rock discontinuities to measure the shear strength, the surfaces roughness, and their progressive damage during shearing process. The progressive discontinuity damage and the consequently loss of shear strength is mainly due to the degradation of fracture asperities [12], influenced by many factors and especially by the normal confinement stress acting along the discontinuity surface.

In this study, direct shear tests were performed on nine natural rock joint specimens of three different lithotypes. The results of these tests allowed to define the peak and residual resistance conditions measured after five shearing cycles. In order to analyse the evolution of the asperities damage during the shearing process the morphology of both the discontinuity surfaces were measured by a photogrammetric survey in three different conditions: intact surfaces (before the test), after the first shearing action (at the end of the first cycle), and at the ultimate conditions (after the 5<sup>th</sup> cycle). Photogrammetric survey allowed the reconstruction of the digital surface model (DSM) processed along several linear profiles, to get roughness geometric descriptors and their statistical variation along the entire surfaces. The results have been used for a JRC assessment by using empirical correlations [13]. The comparison between the experimental results and the roughness surface direct measure allowed to obtain useful information to quantify the discontinuity degree of damage in relation to the state of confinement induced during the tests.

## 2. Shear tests

The shear tests were conducted at the laboratory of the Department of Earth Sciences "Ardito Desio" University of Milan. The tests were performed on three lithotypes for a total of nine samples: three samples of rhyodacites called G1, G2 and G3; three marble samples M1, M2 and M3 and three samples of paragneiss C1, C2 and C3.

The shear tests were carried out through a direct simple shear apparatus on samples having average dimension of 80 mm x 100 mm, imposing a constant value of the normal confinement stress, and controlling the shear load rate. The displacements induced during the tests have been measured by five linear variable displacement transducers: 4 verticals to measure normal displacements and 1 horizontal to measure the shearing displacement. The load and displacement have been controlled and measured by an automatic acquisition system. The three samples belong to each lithotype have been tested imposing three different constant value of the normal stress (1.5, 2.5 and 4 MPa) and five shearing cycles.

The shear test was divided into different phases:

1. Confinement phase ( $\sigma_n$ ): each normal confinement level has been reached imposing a step by step increasing (0.5 MPa each) and measuring the normal displacement induced and the relative discontinuity normal stiffness ( $Kn$ ).
2. Shear phase ( $\tau$ ): once the normal confinement reference value was reached the shear load was imposed with a constant rate until a maximum shear displacement of 120 mm.
3. After this first cycle the sample has been repositioned in the initial configuration, the vertical confinement load applied, and the shear load imposed in order to carried out further four shearing cycles.

## 3. Photogrammetric survey

The intact surfaces (before the shearing tests) and the damaged ones (after the first and the fifth cycles) the discontinuity surfaces were object of a photogrammetric survey to reproduce their morphology toward a DSM and analyse their progressive degradation during the shear tests.

The purpose of this procedure is to obtain a measure of the progressive roughness degradation which, at the laboratory scale, corresponds to a very small variation in the asperities' height (usually less than one millimetre). In order to maximise the accuracy obtainable during the acquisition process, a reference net point with a spacing of 30 mm, carved by laser ray in a rectangular mask in hollow brass, was used and perfectly connected to the shear box (Figure 1a). After placing the mask and illuminating the discontinuity surfaces, a series of 12 shots suitably rotated were taken by using a NIKON D800 (50 mm focal length and 36,3 MP CMOS Full-Frame sensor).

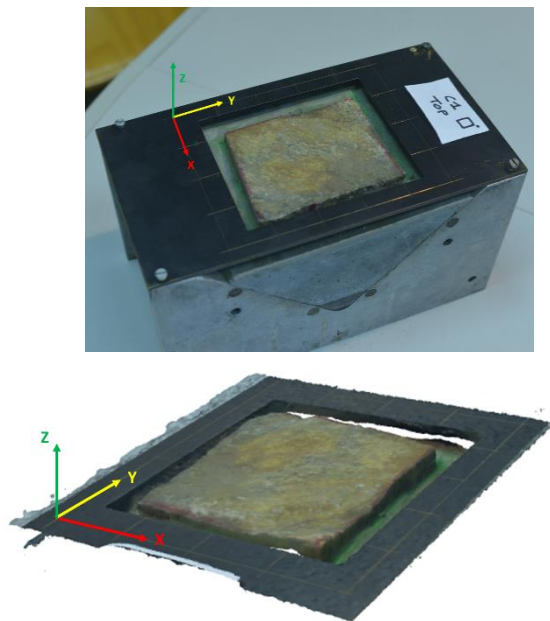


**Figure 1.** Image processing with AM software: (a) shot with reference system indication; (b) example of DSM reconstruction.

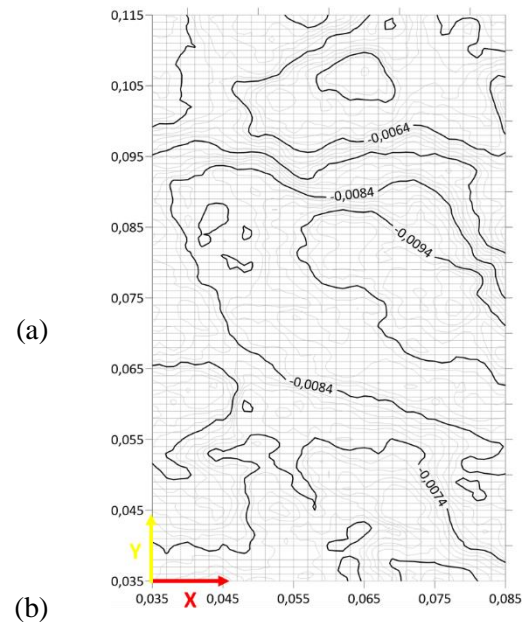


**Figure 2.** Example of a regular grid with contour lines generated with Surfer software.

The digital images taken have been elaborated with Agisoft Metashape software [14], in order to obtain 54 Points clouds and the relative DSMs (Figure 1b): 3 lithotypes, 3 samples for each lithotype, 3 damage degrees and two surfaces for each sample (Top and Bottom surfaces). The points belonging to the discontinuity surface were represented respect to a specific reference system: X and Y axes belong to the horizontal shearing plane where Y is directed as the shearing direction; Z is the vertical one and represents the asperities height respect to a reference plane. The errors in locating the control points in the three coordinates are about 0.07 mm in X and Y directions, 0.1 mm in Z direction.

In order to analyse the surface roughness along linear profiles it is necessary to transform the cloud of irregularly scattered points obtained by the photo-processing into a regular points grid in the XY plane. With this purpose the scattered point clouds have been processed with Surfer® software [15], by extrapolating the height data (Z coordinate) according by a regular grid of points (Figure 2). Only the central portion of the surfaces have been analysed considering a grid with a dimension of 50x80 mm and a point spacing of 1 mm along the x direction and of 0.5 mm along the y direction. For each surface 51 profiles were reconstructed with a length of 80 mm

## 4. Results

### 4.1. Shear tests results

During the shear tests, measurements of normal and shear stresses and displacements were taken at all stages of the test. This allowed to determine the value of shear stiffness ( $K_s$ ), defined by the ratio

between the peak shear stress and its corresponding shear displacement, and the normal stiffness ( $K_n$ ), as the ratio of normal stress to normal displacement, computed in the first test phase.

In the first cycle of shear phase all the samples showed a typical peak-residual behaviour which is dampened considerably in the subsequent cycles. Figure 3 shows the shear stress vs shear displacement curves for the three paragneiss samples as an example.

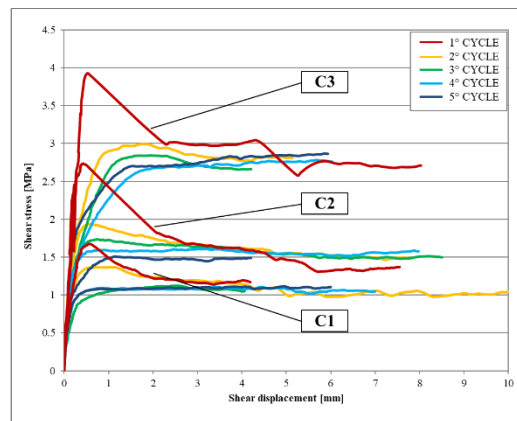
Table 1 shows the results obtained for all samples in terms of normal confinement stress ( $\sigma_n$ ), peak shear stress ( $\tau_p$ ), residual shear stress ( $\tau_r$ ), shear stress variation between the peak and residual value ( $\Delta\tau$ ), shear displacement at shear peak ( $s_p$ ), shear stiffness ( $K_s$ ), normal displacement reached at the end of the confinement phase ( $s_n$ ) and normal stiffness ( $K_n$ ).

Figure 4 shows, in the normal stress vs shear stress plane, the results obtained for paragneiss samples in the first, second and last cycles.

**Table 1.** Results of the shear test for nine samples.

| Lithotype   | Sample | $\sigma_n$<br>[MPa] | $\tau_p$<br>[MPa] | $\tau_r$<br>[MPa] | $\Delta\tau$<br>[MPa] | $s_p$<br>[mm] | $K_s$<br>[MPa/mm] | $s_n$<br>[mm] | $K_n$<br>[MPa/mm] |
|-------------|--------|---------------------|-------------------|-------------------|-----------------------|---------------|-------------------|---------------|-------------------|
| Paragneiss  | C1     | 1.50                | 1.67              | 1.14              | 0.54                  | 0.56          | 4.39              | 0.22          | 9.42              |
|             | C2     | 2.50                | 2.74              | 1.31              | 1.43                  | 0.42          | 12.95             | 0.29          | 11.87             |
|             | C3     | 4.00                | 3.93              | 2.58              | 1.35                  | 0.54          | 9.21              | 1.50          | 6.89              |
| Rhyodacites | G1     | 1.55                | 2.29              | 1.94              | 0.36                  | 1.71          | 2.01              | \             | \                 |
|             | G2     | 2.89                | 3.94              | 3.22              | 0.72                  | 1.23          | 3.72              | 0.60          | 13.60             |
|             | G3     | 5.39                | 6.84              | 5.06              | 1.78                  | 1.62          | 4.18              | 0.80          | 16.80             |
| Marble      | M1     | 1.50                | 1.15              | 0.46              | 0.69                  | 1.53          | 1.17              | 0.28          | 7.65              |
|             | M2     | 2.50                | 2.31              | 1.50              | 0.81                  | 0.94          | 2.75              | 0.84          | 7.23              |
|             | M3     | 4.00                | 3.59              | 2.03              | 1.56                  | 1.20          | 3.22              | 1.00          | 12.23             |

Note: "\" data missing due to no-data acquisition



**Figure 3.** Shear behaviour along the discontinuities referred to the five cycles for samples C1, C2 and C3.

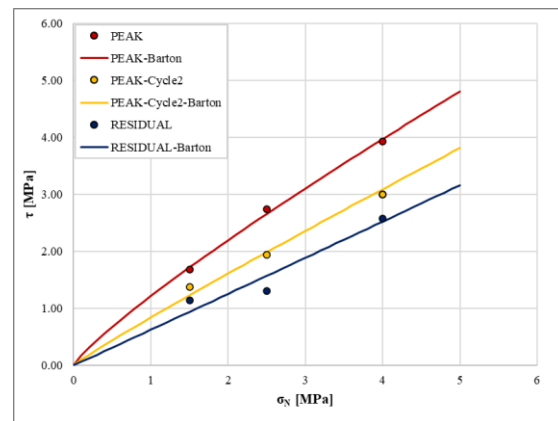


**Figure 4.** Back-analysis of experimental data using Barton's criterion for samples C1, C2 and C3.

The results of the shear tests provide experimental data to reconstruct the mechanical behaviour of discontinuities. The residual data were analysed using the Mohr-Coulomb resistance criterion (1) while the peak data with Barton's criterion (2), as follows [2] (Figure 4):

$$\tau = c + \sigma_n \tan \varphi \quad (1)$$

$$\tau_p = \sigma_n \tan \left[ \varphi_r + JRC \cdot \text{Log}_{10} \left( \frac{JCS}{\sigma_n} \right) \right] \quad (2)$$

A  $JRC_{lab}$  value for each lithotype was obtained by a back analysis considering the best fit curve of the experimental data by using equation (2) for the three reference cycles; with this purpose, the residual

resistance angle ( $\varphi_r$ ) was defined by the analysis of residual results and the Joint Compressive Strength JCS value determined through sclerometric tests (Table 2). In order to study the damage process on each sample, the Barton's equation was applied to the results obtained at the three reference cycles for each sample ( $JRC_{single}$ ).

**Table 2.** JRC values obtained from the interpolation of the experimental data for the nine samples.

| Lithotype   | $\varphi_r$<br>[°] | JCS<br>[MPa] | Sample | Cycle 1       |            | Cycle 2       |            | Cycle 5       |            |
|-------------|--------------------|--------------|--------|---------------|------------|---------------|------------|---------------|------------|
|             |                    |              |        | JRC<br>single | JRC<br>lab | JRC<br>single | JRC<br>lab | JRC<br>single | JRC<br>lab |
| Paragneiss  | 33                 | 69.7         | C1     | 9.12          |            | 5.65          |            | 2.56          |            |
|             |                    |              | C2     | 10.12         | 9.51       | 3.36          | 4.04       | 0.00          | 0.85       |
|             |                    |              | C3     | 9.28          |            | 3.11          |            | 0.00          |            |
| Rhyodacites | 44                 | 52.5         | G1     | 7.60          |            | 5.91          |            | 3.10          |            |
|             |                    |              | G2     | 7.52          | 7.55       | 3.65          | 3.68       | 2.59          | 1.90       |
|             |                    |              | G3     | 7.53          |            | 1.48          |            | 0.00          |            |
| Marble      | 32.5               | 155          | M1     | 2.49          |            | 1.38          |            | 0.00          |            |
|             |                    |              | M2     | 5.73          | 4.72       | 3.25          | 1.73       | 0.00          | 0.00       |
|             |                    |              | M3     | 5.95          |            | 0.56          |            | 0.00          |            |

#### 4.2. Processing of photogrammetric survey results

Each profile obtained through the analysis with Surfer was analysed in order to obtain a roughness measurement through the  $Z_2$  parameter [16]:

$$Z_2 = \left[ \frac{1}{N(d_y)^2} \sum_{i=1}^N (z_{i+1} - z_i)^2 \right]^{\frac{1}{2}} \quad (3)$$

where  $N$  is the number of measurements along  $y$ ,  $d_y$  is the scanning step and  $z$  is the profile elevation respect to an average plane.

For each surface, 51 profiles were analysed allowing a statistical analysis of the roughness variation along the surfaces in the three shearing cycles.

To evaluate and compare the roughness estimated through photogrammetric analysis and that one evaluated with mechanical analysis, it is necessary to choose a correlation between the statistical parameter  $Z_2$  with the JRC coefficient. In this work, among the different correlations proposed in the literature, the one proposed by Tse & Cruden [13] reported in the following equation (4) was used.

$$JRC = 32.2 + 32.47 \cdot \log(Z_2) \quad (4)$$

Using this correlation, it is possible to obtain value of JRC for each profile and then carried out frequency analysis. As an example, the Figure 5 shows the frequency distributions for the C2 sample in the pre-shearing, post-shearing and residual conditions. The red solid line represents the JRC frequency distribution of the lower sample surface, while the blue solid line represents the upper one, the dashed lines represent the average value of the two distributions, and the grey solid line represents the JRC lab value.

It can be observed that the frequency distribution shows an inhomogeneity of the surface roughness highlighting in this case a bimodal behaviour. In the first cycle JRC varies between 0 and 10 in the second between 0 and 7 and in the last cycle between 0 and 6.

After the first (Cycle 1) and the last shearing cycle (Cycle 5) a significant decrease in roughness is observed: the frequencies of the higher values of JRC decrease and those of the lower values increase.

It is clear from the graphs that the average JCR values are not representative of the roughness of the sample. In fact, the C2 sample has a bimodal distribution and the average value of JRC falls into a class with a lower frequency compared to that of the two peaks.

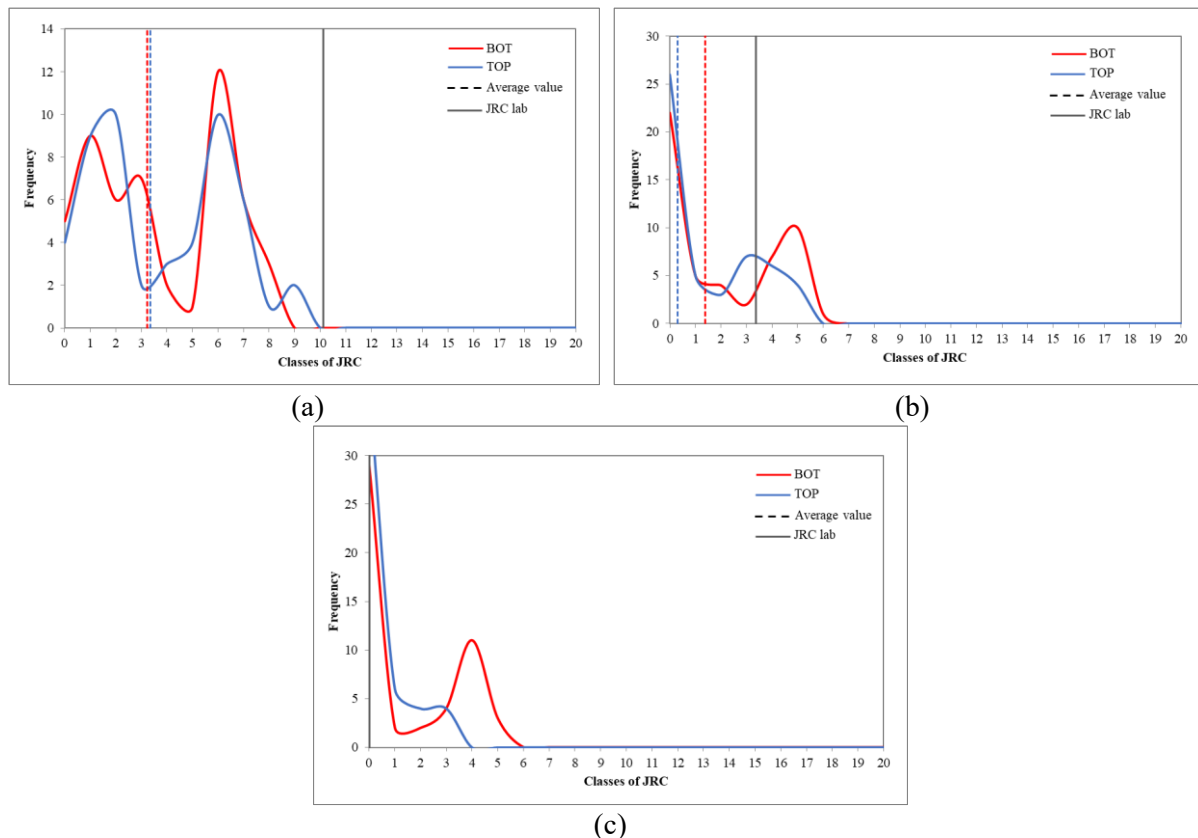


**Figure 5.** JRC frequency distributions for the C2 sample in the pre-shearing (a), post-shearing (b) and residual conditions (c).

The Table 3 summarizes the results obtained for the nine samples considering for each sample the average value of the frequency distributions of the two halves "TOP" and "BOT". As you can see, the JRC values do not correspond to those obtained with the mechanical analysis and this because, in most cases, the average value is not representative of the roughness of the samples.

**Table 3.** JRC values obtained from photogrammetric analysis compared with those obtained laboratory tests.

| Lithotype   | Sample | Cycle 1    |             |         | Cycle 2    |         |         | Cycle 5    |         |         |
|-------------|--------|------------|-------------|---------|------------|---------|---------|------------|---------|---------|
|             |        | JRC single | JRC average | JRC lab | JRC single | JRC med | JRC lab | JRC single | JRC med | JRC lab |
| Paragneiss  | C1     | 6.72       |             |         | 5.84       |         |         | 4.99       |         |         |
|             | C2     | 3.29       | 4.70        | 9.51    | 0.84       | 2.99    | 4.04    | 0.00       | 1.88    | 0.85    |
|             | C3     | 4.10       |             |         | 2.28       |         |         | 0.66       |         |         |
| Rhyodacites | G1     | 13.61      |             |         | 7.41       |         |         | 5.03       |         |         |
|             | G2     | 16.30      | 13.27       | 7.55    | 5.04       | 6.29    | 3.68    | 2.02       | 3.50    | 1.90    |
|             | G3     | 9.91       |             |         | 6.43       |         |         | 3.44       |         |         |
| Marble      | M1     | 0.42       |             |         | 0.11       |         |         | 0.00       |         |         |
|             | M2     | 0.94       | 1.47        | 4.72    | 0.41       | 1.03    | 1.73    | 0.00       | 0.65    | 0.00    |
|             | M3     | 3.94       |             |         | 2.57       |         |         | 1.94       |         |         |

#### 4.3. Discontinuity degree of damage in relation to the state of confinement

It is well known that the peak resistance is related to the roughness of the surface: the peak strength increases with the surface roughness and confinement stress increasing. Similarly, the strength drop in the post-peak phase is related to a progressive asperities' degradation due to the friction forces during the shearing. Under the same initial roughness conditions, the drop in resistance is greater the higher is the normal confinement value, since the greater the degree of damage due to friction of the asperities present should be. This is evident from the results of the laboratory tests reported in Table 1 where it is observed that the drop in resistance between peak and residue in the first cycle ( $\Delta\tau$ ) is strictly affected by the normal stress applied. In fact, due to the increase in normal stress, more complete contact can be made between the upper and lower parts of the joint surface. This phenomenon results in a substantial reduction in the JRC value during the shearing phase.

To analyse the effect of normal stress on rock joint surface degradation, a degradation factor FD was defined as ratio of JRC variation to the initial JRC:

$$FD = \frac{\Delta JRC}{JRC_0} = \frac{JRC_0 - JRC_1}{JRC_0} \quad (5)$$

where the JRC variation ( $\Delta JRC$ ) is the difference between intact ( $JRC_0$ ) and degraded discontinuity after the first shearing cycle ( $JRC_1$ ) and it was calculated for each sample and at different confinement stress.

Figure 6 reports the results in terms of FD and  $\sigma_n$  obtained both from laboratory tests and photogrammetric analysis. Comparing the results of the JRC variation with the tensional data of the first shearing cycle of each sample it is observed that an increasing of  $\sigma_n$  corresponds to a growth in the degradation factor.

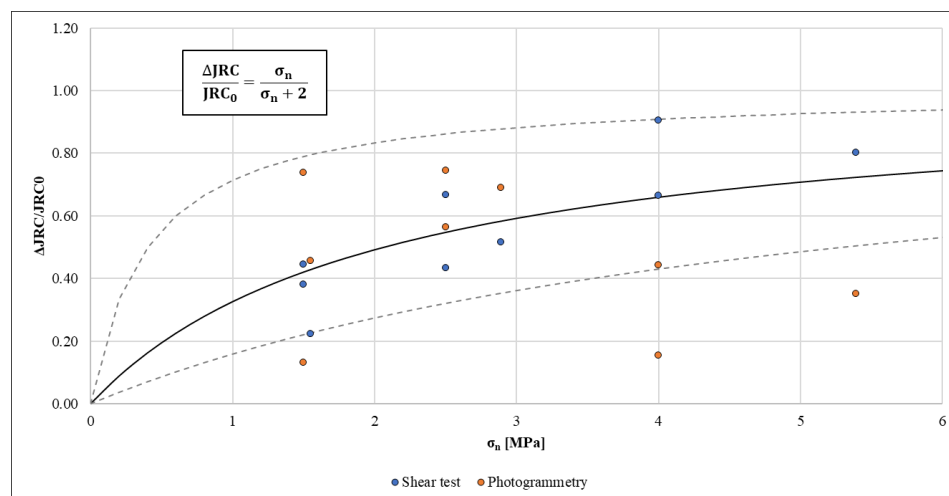


**Figure 6.** Data analysis in terms of degradation factor respect to the applied confinement state.

Through a least square analysis it was possible to define the function that best interpolates the results obtained with which the degradation factor is defined as a function of the level of confinement of the sample. The obtained function is reported in the following equation (6):

$$FD = \frac{\sigma_n}{\sigma_n + 2} \quad (6)$$



## 5. Conclusion

The paper describes an experimental procedure carried out at laboratory scale on natural rock discontinuities to measure the shear strength, the surfaces roughness, and their progressive damage during shearing process.

In that sense, photogrammetric techniques have turned out to be a useful tool that allows to analyse the discontinuity surfaces to obtain geometric descriptors able to numerically describe the degree of roughness of the surface. However, the comparison of the JRC' estimation resulting from back analysis of experimental tests and measurements made on discontinuities has shown that discontinuities, even at the small scale, have an inhomogeneous roughness, which should be analysed as surface roughness. In fact, from the photogrammetric analysis bimodal frequency distributions were obtained and for this reason it was not possible to define the representative value of the roughness of the samples.

The photogrammetric analysis of the surfaces in the different shearing cycles allowed to study the degradation of the joint surface and the factors that influence it. In fact, the results obtained allowed to analyse the degradation factor of the surface, highlighting that degradation is a progressive process strongly influenced by the degree of confinement of the sample.

## References

- [1] Patton FD 1966 Multiple modes of shear failure in rock Proc. *1st ISRM Congress Int. Society for Rock Mech. Rock Eng. (Lisbon)* 25 September-1 October
- [2] Barton N and Choubey V 1977 The shear strength of rock joints in theory and practice *Rock Mech.* **10 (1-2)** 1–55
- [3] Castelli M, Re F, Scavia C and Zaninetti A 2001 Experimental evaluation of scale effects on the mechanical behavior of rock joints Proc. *EUROCK 2001 Rock Mechanics, A Challenge for Society (Espoo, Finland)* 3–7 June
- [4] Bandis S 1980 Experimental studies of scale effects on shear strength, and deformation of rock joints *Ph.D. thesis, Uni of Leeds (Leeds, UK)*
- [5] Cruden DM and Hu XQ 1988 Basic friction angles of carbonate rocks from Kananaskis country, Canada *Bull. Int. Assoc. Eng. Geol.* **38** 55–59
- [6] Özvan A, Dinçer İ, Acar A and Özvan B 2013 The effects of discontinuity surface roughness on the shear strength of weathered granite joints *Bull. Eng. Geol. Environ.* **73**, 801–813
- [7] Ferrero AM, Migliazza M and Tebaldi G 2010 Development of a new experimental apparatus for the study of the mechanical behaviour of a rock discontinuity under monotonic and cyclic loads *Rock. Mech. Rock. Eng.* **43 (6)** 685–695
- [8] Li Y and Zhang Y 2015 Quantitative estimation of joint roughness coefficient using statistical parameter *Int. J. Rock Mech. Min. Sci.* **77** 27–35
- [9] Ferrero AM, Migliazza MR and Umili G 2019 Comparison of methods for discontinuity roughness evaluation *RIVISTA ITALIANA DI GEOTECNICA* **3** 5-15
- [10] Li Y and Huang R 2015 Relationship between joint roughness coefficient and fractal dimension of rock fracture surfaces *Int. J. Rock Mech. Min. Sci.* **75 (15)** 15–22
- [11] Wernecke C and Marsch K 2015 Mapping rock surface roughness with photogrammetry *EUROCK 2015 (Salzburg)* October 7–10
- [12] Lee HS, Park YJ, Cho TF and You KH 2001 Influence of asperity degradation on the mechanical behavior of rough rock joints under cyclic shear loading *Int. J. Rock. Mech. Min. Sci.* **38 (7)** 967–980
- [13] Tse R and Cruden DM 1979 Estimating joint roughness coefficients *Int. J. Rock Mech. Min. Sci. Geomech. Abstr.* **16 (5)** 303–307
- [14] Agisoft Metashape User Manual, Professional Edition, version 1.7.4
- [15] Surfer® from Golden Software, LLC version 16
- [16] Myers NO 1962 Characterization of surface roughness *Wear* **5 (3)** 182–189